

## The Time of Flight Detector at CDF

C.Grozis<sup>a</sup>, R.Kephart<sup>a</sup>, R.Stanek<sup>a</sup>, B.Kim<sup>b</sup>, D.H.Kim<sup>b</sup>, S.B.Kim<sup>b</sup>, Y.Oh<sup>b</sup>, I.Yu<sup>b</sup>, W.Carithers<sup>c</sup>, Y.K.Kim<sup>c</sup>, K.Anikeev<sup>d</sup>, G.Bauer<sup>d</sup>, I.K.Furić<sup>d</sup>, A.Korn<sup>d</sup>, I.Kravchenko<sup>d</sup>, M.Mulhearn<sup>d</sup>, Ch.Paus<sup>d</sup>, S.Pavlon<sup>d</sup>, K.Sumorok<sup>d</sup>, S.Cabrera<sup>e</sup>, T.Rodrigo<sup>e</sup>, A.Ruiz<sup>e</sup>, I.Vila<sup>e</sup>, C.Chen<sup>f</sup>, M.Jones<sup>f</sup>, W.Kononenko<sup>f</sup>, J.Kroll<sup>f</sup>, G.M.Mayers<sup>f</sup>, F.M.Newcomer<sup>f</sup>, D.Usynin<sup>f</sup>, R.Van Berg<sup>f</sup>, G.Bellettini<sup>g</sup>, C.Cerri<sup>g</sup>, A.Menzione<sup>g</sup>, D.Depedis<sup>h</sup>, C.Dionisi<sup>h</sup>, S.Giagu<sup>h</sup>, M.Rescigno<sup>h</sup>, L.Zanello<sup>h</sup>, A.Kazama<sup>i</sup>, S.H.Kim<sup>i</sup>, H.Matsunaga<sup>i</sup>, S.Motohashi<sup>i</sup>, K.Sato<sup>i</sup>, K.Takikawa<sup>i</sup>, F.Ukegawa<sup>i</sup>

<sup>a</sup>Fermi National Laboratory

<sup>b</sup>Korea Hadron Collider Laboratory

<sup>c</sup>Lawrence Berkeley National Laboratory

<sup>d</sup>Massachusetts Institute of Technology

<sup>e</sup>IFCA (CSIC-Univ. Cantabria)

<sup>f</sup>University of Pennsylvania

<sup>g</sup>INFN, University of Pisa

<sup>h</sup>INFN, University of Rome1, La Sapienza

<sup>i</sup>University of Tsukuba

A Time-of-Flight detector (TOF) has been incorporated into the CDF-II experiment in order to provide charged kaon identification to improve neutral B meson flavor determination. With an expected time-of-flight resolution of 100 ps, the system will be able to provide 2 standard deviation separation between  $K^\pm$  and  $\pi^\pm$  for momenta  $p < 1.6$  GeV/c, complementing the specific ionization energy loss  $dE/dx$  measured with the new drift chamber.

### 1. Introduction

During the Run I data taking period from 1992 to 1996 the CDF experiment at the Fermilab Tevatron accelerator ( $\sqrt{s} = 1.8$  TeV) accumulated an integrated luminosity of  $110 \text{ pb}^{-1}$ . Following Run I, the CDF detector has been substantially upgraded for the next data collection period Run II of the Tevatron [1]. The goal of the Tevatron is to deliver  $2 \text{ fb}^{-1}$  at  $\sqrt{s} = 2.0$  TeV in the first two years and more than  $15 \text{ fb}^{-1}$  in 5 years of running.

A time-of-flight (TOF) system is being added to the detector [2] to improve the particle identification capability. The TOF was the most practical enhancement given the constraints of space

and cost.

The primary purpose of the TOF is to identify the  $b$  flavor of B hadrons produced in the collisions. An enhancement of the  $b$  flavor identification is crucial to improve the statistical precision in CP violation measurements and  $B_s^0 - \bar{B}_s^0$  oscillations [1–3].

### 2. Flavor tagging with TOF

The TOF system will play a crucial role in determining the  $b$  flavor (content of  $b$  or  $\bar{b}$ ) of B mesons. CDF developed several methods of  $b$  flavor determination or “tagging” during Run I; in Run II these methods will be extended and new methods will be added. The figure of merit to

quantify the power of a  $b$  flavor tag is the “total tag effectiveness”  $\epsilon\mathcal{D}^2$ , where  $\epsilon$  is the tag efficiency and  $\mathcal{D}$  is the tag dilution, which is related to the probability  $\mathcal{P}$  that the flavor tag is correct:  $\mathcal{D}=2\mathcal{P}-1$ . The statistical error of a CP asymmetry is proportional to  $1/\sqrt{\epsilon\mathcal{D}^2}$ ; in addition the statistical significance of a measurement of an oscillation frequency is proportional to  $\sqrt{\epsilon\mathcal{D}^2}$ .

There are two types of flavor tags: *opposite side tags*, which are based on identifying the flavor of the second B hadron in the collision to infer the flavor of the B hadron of interest, and *same side tags*, which exploit the charge correlation of particles produced in association with the hadronization of a  $b$  quark into a B meson. The identification of a charged kaon can be used as an opposite side tag, since  $\overline{B}$  hadrons produce more  $K^-$  than  $K^+$  on average through the decay sequence  $b \rightarrow c \rightarrow s$ . Kaon identification also enhances the effectiveness in the same side tagging. In particular, a  $B_s^0$  ( $\overline{B}_s^0$ ) will be produced in association with a  $K^+$  ( $K^-$ ).

The opposite side kaon tag was not established in Run I. Figure 1 shows that a significant fraction of kaons from the second B hadron are in the identification range of the TOF. Combined with the same side kaon tag, the TOF is expected to double the flavor tag effectiveness for  $B_s^0/\overline{B}_s^0$  mesons (see table 1).

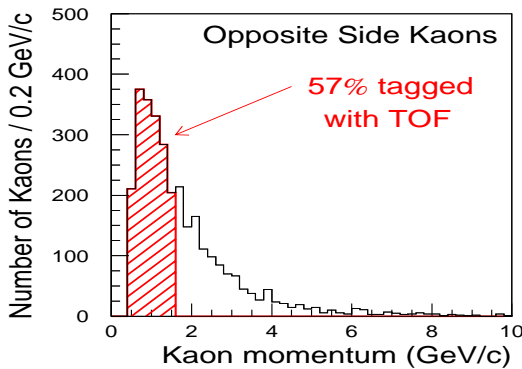


Figure 1. Momentum spectrum of kaons from the B decay opposite the reconstructed  $B^0/\overline{B}^0 \rightarrow J/\psi K_s^0$ .

## 2.1. Kaon identification

Particle identification with the TOF is performed by measuring the difference (time-of-flight) in the time of arrival of the particle at the scintillator with the collision time  $t_0$ . The mass  $m$  can be determined from the momentum  $p$ , the path-length  $L$ , and the time-of-flight  $t$ :

$$m = \frac{p}{c} \cdot \sqrt{\frac{c^2 t^2}{L^2} - 1},$$

where  $p$  and  $L$  are measured by the tracking system. Figure 2 shows the time-of-flight difference between  $K/\pi$ ,  $p/K$  and  $p/\pi$ . The average statistical separation is shown as well assuming a time-of-flight resolution of 100 ps. For comparison the separation provided by  $dE/dx$  is shown too; the TOF improves substantially  $K/\pi$  separation in the critical momentum region  $p < 1.6$  GeV/c.

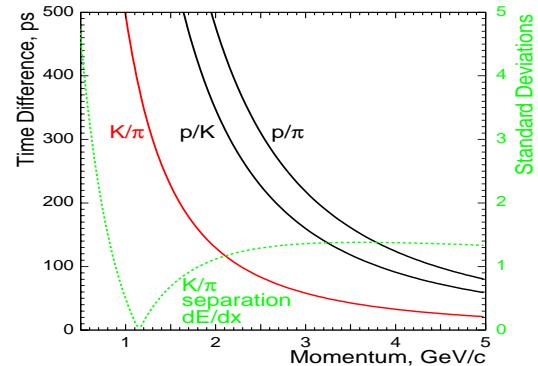


Figure 2. The time-of-flight difference (in ps) between  $K/\pi$ ,  $p/\pi$  and  $K/p$ .

## 3. The TOF system

The TOF detector consists of 216 bars of Bicron BC-408 scintillator, which was selected for its long attenuation length ( $\Lambda_{\text{eff}} \sim 250$  cm) and fast rise time. The bar dimensions are 279 cm  $\times$  4 cm  $\times$  4 cm. They are installed at a radius of  $\sim 138$  cm from the beam in the 4.7 cm of radial space between the main drift chamber and the cryostat of the superconducting solenoid. The material thickness of tracking systems before the

Table 1

Projected values for  $\epsilon\mathcal{D}^2$  for Run II with and without TOF. The difference in same side tagging effectiveness for the two  $B_s^0$  decay modes is due to the trigger.

$B^0/\bar{B}^0 \rightarrow J/\psi K_S^0$	without TOF	with TOF
Same-Side (pion) Tag	1.4	1.9
Opposite-Side Kaon Tag	–	2.4
$B_s^0/\bar{B}_s^0 \rightarrow J/\psi \phi$	without TOF	with TOF
Same-Side (kaon) Tag	0.2	2.6
Opposite-Side Kaon Tag	–	2.4
$B_s^0 \rightarrow D_s^+ \pi^+$	without TOF	with TOF
Same-Side (kaon) Tag	1.0	4.2
Opposite-Side Kaon Tag	–	2.4

TOF is less than 10%  $X_0$ . The pseudo-rapidity coverage of the system is roughly  $|\eta| < 1$ .

### 3.1. The photomultipliers: features and assembly

A Hamamatsu R7761, 19-stage, fine mesh [4] photomultiplier tube (PMT) is attached to each end of the scintillator bars for a total of 432 PMTs in the system. These tubes can operate in the 1.4 T magnetic field produced by the CDF solenoid, but with reduced gain. An initial analysis of the performance of the tubes indicated an intrinsic timing resolution better than 100 ps and an average gain reduction factor of 500 in a 1.4 T magnetic field. The tubes may operate at positive voltages up to 2500 V and exhibit very stable gains in the magnetic field.

The PMTs form part of an assembly that is contained in aluminum holders that are attached to the end of the scintillator. This scheme allowed installation of the PMTs after the bars were installed on the detector and makes it possible to replace a PMT that fails during data taking. The PMT assembly (see figure 3) consists of a parabolic compact light concentrator (Winston Cone) that focuses the light from the maximal diameter of 1.5 inches onto the sensitive area of the photocathode; a Bicon silicone pad that provides the optical contact between the cone and the scintillator; the PMT itself; the PMT base; the preamplifier; a spring that ensures good optical contact between the scintillator and the cone;

and a cap containing a printed circuit board for high voltage, low voltage, and signal connections.



Figure 3. A photograph of the PMT assembly.

### 3.2. The electronics

A custom designed high voltage base is attached to the PMTs. The differential signal formed from the anode and the last dynode stage of the PMT is fed through a preamplifier, which drives a differential signal over 10 m of cable to the front end electronics. There the signal follows two paths, one for the timing measurement, and the second for a charge measurement. In the first path, the signal is fed into a leading edge discriminator and the output serves as the start sig-

nal for the Time to Amplitude Conversion (TAC) circuit. The TAC is stopped by a common stop signal produced by a precision clock with an expected jitter less than 25 ps. In the second path a gated integration of the charge of the pulse is used to correct the time measurement for pulse height dependence.

#### 4. Results from the prototype and conclusions

A TOF test system with 20 130 cm bars was installed inside the CDF solenoid at the end of the Run I to learn how to achieve the best timing resolution (100 ps) from a full system [5]. From a fit to the TOF mass spectrum of the data (see figure 4) the flight time resolution averaged over all the tubes was 220-250 ps. The low resolution was mainly due to: reduced statistics (only 5% coverage), resulting in a poor resolution in the  $t_0$  determination, reduced statistics for the time-slewing correction, some broken joints in the coupling between the PMTs and the scintillator, and very low amplitude signals in the 16-stage PMTs within the 1.4 T magnetic field. These problems are addressed in the design of the full system. Using cosmic ray muons, a resolution of about 110 ps has been obtained with 16-stage PMTs. The 19-stage PMTs show a comparable timing performance.

A track matching efficiency about 95%, and an occupancy 10-20% (depending on the luminosity) has been obtained by simulation [6].

#### REFERENCES

1. The CDFII Collaboration, R. Blair *et al.*, The CDF II Detector Technical Design Report, FERMILAB-PUB-96/390-E.
2. The CDF-II Coll.: *Proposal for enhancement of the CDF-II Detector: an Inner Silicon Layer and Time of Flight Detector (P-909)*, <http://www-cdf.fnal.gov/upgrades/btb.proposal.ps>  
Update to proposal P-909: *Physics Performance of the CDF-II with an Inner Silicon Layer and a Time of Flight Detector*, [http://www-cdf.fnal.gov/upgrades/btb\\_update\\_jan99.ps](http://www-cdf.fnal.gov/upgrades/btb_update_jan99.ps)

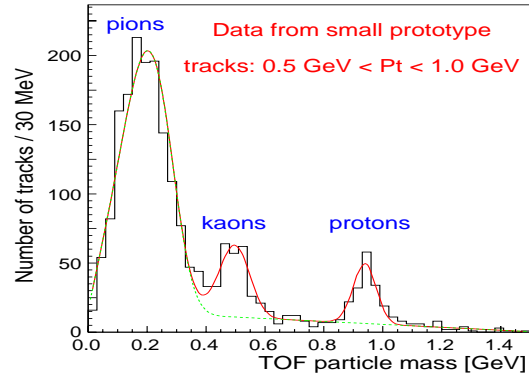


Figure 4. The measured TOF mass spectrum with the TOF prototype. The solid line is a fit that includes contributions from pions, kaons, protons, and a linear background.

3. A. Ruiz, these proceedings.
4. "Photomultiplier tube: principle to application" Ed. Hamamatsu Photonics K.K. editorial committee, 1994.
5. F.Ukegawa et al.: Nucl. Instr. and Meth., A439 (2000), 65-79.
6. C. Paus for the TOF group of CDF II, 8th Pisa Meeting on advanced detector 21-27 May 2000.